IOP PUBLISHING PHYSICS IN MEDICINE AND BIOLOGY

Phys. Med. Biol. **54** (2009) 3141–3159 doi:10.1088/0031-9155/54/10/012

Computed tomography dose assessment for a 160 mm wide, 320 detector row, cone beam CT scanner

J Geleijns[1], M Salvadó Artells[2], P W de Bruin[1], R Mather[3], Y Muramatsu[4] and M F McNitt-Gray[5]

[1] Radiology Department, Leiden University Medical Center, Albinusdreef 2, 2333 ZA Leiden, The Netherlands
[2] Rovira i Virgili University, Faculty of Medicine and Health Sciences, C/Sant Llorenç 21, 43201 Reus, Spain
[3] Toshiba America Medical Systems, Inc., 2441 Michelle Drive, Tustin, CA 92780, USA
[4] Radiology Department, National Saitama Hospital, 2-1, Suwa, Wako, Saitama, Japan
[5] Department of Radiological Sciences, David Geffen School of Medicine at UCLA, Thoracic Imaging Research Group, 924 Westwood Blvd, Suite 650, Los Angeles, CA 90024, USA

E-mail: K.Geleijns@lumc.nl

Received 7 January 2009, in final form 20 March 2009
Published 6 May 2009
Online at stacks.iop.org/PMB/54/3141

Abstract

Computed tomography (CT) dosimetry should be adapted to the rapid developments in CT technology. Recently a 160 mm wide, 320 detector row, cone beam CT scanner that challenges the existing Computed Tomography Dose Index (CTDI) dosimetry paradigm was introduced. The purpose of this study was to assess dosimetric characteristics of this cone beam scanner, to study the appropriateness of existing CT dose metrics and to suggest a pragmatic approach for CT dosimetry for cone beam scanners. Dose measurements with a small Farmer-type ionization chamber and with 100 mm and 300 mm long pencil ionization chambers were performed free in air to characterize the cone beam. According to the most common dose metric in CT, namely CTDI, measurements were also performed in 150 mm and 350 mm long CT head and CT body dose phantoms with 100 mm and 300 mm long pencil ionization chambers, respectively. To explore effects that cannot be measured with ionization chambers, Monte Carlo (MC) simulations of the dose distribution in 150 mm, 350 mm and 700 mm long CT head and CT body phantoms were performed. To overcome inconsistencies in the definition of $CTDI_{100}$ for the 160 mm wide cone beam CT scanner, doses were also expressed as the average absorbed dose within the pencil chamber ($\overline{D}_{100}$). Measurements free in air revealed excellent correspondence between $CTDI_{300air}$ and $\overline{D}_{100air}$, while $CTDI_{100air}$ substantially underestimates $CTDI_{300air}$. Results of measurements in CT dose phantoms and corresponding MC simulations at centre and peripheral positions were weighted and revealed good agreement between $CTDI_{300w}$, $\overline{D}_{100w}$ and $CTDI_{600w}$, while $CTDI_{100w}$ substantially underestimates $CTDI_{300w}$.

$\overline{D}_{100w}$ provides a pragmatic metric for characterizing the dose of the 160 mm wide cone beam CT scanner. This quantity can be measured with the widely available 100 mm pencil ionization chamber within 150 mm long CT dose phantoms. $CTDI_{300w}$ measured in 350 mm long CT dose phantoms serves as an appropriate standard of reference for characterizing the dose of this CT scanner. A CT dose descriptor that is based on an integration length smaller than the actual beam width is preferably expressed as an (average) dose, such as $\overline{D}_{100}$ for the 160 mm wide cone beam CT scanner, and not as $CTDI_{100}$.

(Some figures in this article are in colour only in the electronic version)

1. Introduction

Existing metrics in CT dosimetry should be adapted in order to keep pace with new developments in CT technology. A 320 detector row CT scanner (Aquilion ONE) that challenges the existing Computed Tomography Dose Index (CTDI) dosimetry paradigm was introduced by Toshiba Medical Systems (Otawara-shi, Japan) (Dewey *et al* 2008, Rybicki *et al* 2008). Three hundred and twenty transmission profiles with a nominal section thickness of 0.5 mm can be acquired simultaneously with the Aquilion ONE CT scanner. The scanner is capable of acquisition of a volume that is 160 mm in length, measured along the axis of rotation, in combination with a field of view of 500 mm (in the axial plane), within one 0.35 s full rotation.

Current metrics in CT dosimetry are based on CTDI, and these assume a beam width that is much smaller than the length of the commonly used CT dose phantoms (cylindrical 150 mm long PMMA CT dose head and body phantoms) and much smaller than the length of the standard pencil CT ionization chamber, which has an active length of 100 mm (Shope *et al* 1981). These preconditions are no longer valid for the Aquilion ONE scanner since its maximum nominal beam width of 160 mm exceeds the length of both regular CT dose phantoms and the standard pencil CT ionization chamber. Due to penumbra, the actual beam is slightly wider. Therefore, a modified concept that is compatible with the characteristics of the 160 mm wide cone beam scanner is required. In the longer term, new dosimetric concepts may be developed that are better suited for cone beam CT scanners.

This study aims at providing a pragmatic, but robust and accurate, methodology for dose assessment for the 160 mm wide cone beam CT scanner that is compatible with current dosimetric practices; it provides a framework for acceptance and constancy testing of dose characteristics of the Aquilion ONE CT scanner and for assessment of dosimetric characteristics of this scanner against existing legislation and guidelines. The proposed methodology is based on application of the readily available 150 mm long CT dose phantoms and the 100 mm pencil ionization chamber and on assessment of the full-width half-maximum (FWHM) of the actual cone beam. It is supported by measurements with extended CT dose phantoms and a 300 mm long pencil CT ionization chamber and by Monte Carlo (MC) dose simulations of the dose distribution within 150 mm, 350 mm and 700 mm long CT dose phantoms.

2. Materials and methods

Dose is expressed as absorbed dose in air (mGy). Ionization chambers were appropriately calibrated for the x-ray spectra that they were exposed to; readings were corrected for air temperature and air pressure.

2.1. CT scanner

Dose measurements were performed on a 320 detector row CT scanner (Aquilion ONE). The scanner can be operated at four tube voltages (80 kV, 100 kV, 120 kV and 135 kV) and three different bow tie filters can be selected: bow tie filters for a large (500 mm), a medium (320 mm) and a small scanned field of view (240 mm). This study primarily focuses on dosimetric characteristics of the scanner when it is operated at the largest available nominal beam width (160 mm), covering all 320 detector rows. The effect of collimation on CTDI was assessed for acquisitions with 80–320 active detector rows (in 40 detector row, or 20 mm nominal beam width, steps). Acquisitions with a stationary CT table in combination with either a fixed or rotating x-ray tube were performed. No helical acquisitions were performed since, with the 160 mm extent of anatomical coverage, most clinical acquisitions are expected to be axial scans with a stationary table. Furthermore, in helical mode the Aquilion ONE scanner operates in a regular 64 or less active detector row configuration (each detector row corresponding to 0.5 mm section width) for which existing dose metrics can be applied. Positions relative to the scanner are described by the XYZ frame; the axial plane that coincides with the focal spot is described by the horizontal *X*-axis and vertical *Y*-axis. The horizontal *Z*-axis coincides with the axis of rotation. The focal spot rotates at a distance of 600 mm from the axis of rotation.

2.2. Dose quantities in CT

Currently, the Computed Tomography Dose Index 100 (CTDI_{100}) is the international standard for dose assessment (IEC 60601-2-44 2002). It is defined as a 100 mm long integral of the dose profile along a line perpendicular to the axial (*XY*) plane divided by the product of the nominal section thickness and the number of contiguous sections produced in a single axial scan (FDA 2006, McCollough 2003, McNitt-Gray 2002):

$$\mathrm{CTDI}_{100} = \frac{1}{nT}\int_{-50\ \mathrm{mm}}^{+50\ \mathrm{mm}} D(z)\,\mathrm{d}z \tag{1}$$

where $D(z)$ is the absorbed dose in air at position z, T is the nominal section thickness and n is the number of contiguous sections acquired in a single axial scan. The dose profile should be centred on $z = 0$. CTDI_{100} is originally defined for measurements in CT dosimetry phantoms but CTDI_{100} can also be determined free in air.

The weighted CTDI provides a pragmatic solution for expressing five CTDI values at well-defined positions in a CT dose phantom as one value:

$$\mathrm{CTDI}_w = \tfrac{1}{3} \times \mathrm{CTDI}_{\mathrm{centre}} + \tfrac{2}{3} \times \mathrm{CTDI}_{\mathrm{periphery}} \tag{2}$$

where $\mathrm{CTDI}_{\mathrm{periphery}}$ is the average of CTDI measured at four peripheral positions.

Straightforward application of CTDI_{100} to the 160 mm wide cone beam CT scanner would result in

$$\mathrm{CTDI}_{100} = \frac{1}{160}\int_{-50\ \mathrm{mm}}^{+50\ \mathrm{mm}} D(z)\,\mathrm{d}z \tag{3}$$

where the denominator follows from 320 (active detector rows) × 0.5 (section thickness) mm = 160 mm. An obvious complication occurs from the 160 mm wide cone beam since the 100 mm long integral over $D(z)$ covers only a small part of the actual *Z*-axis dose profile and excludes completely its penumbra and tails of scattered radiation. The denominator *'n.T'*, when taken as 160 mm, exceeds the sensitive length of the 100 mm long pencil ionization chamber which seems to be a violation of the intended use of CTDI, and consequently the large

denominator will result in relatively low values for $CTDI_{100}$. To overcome this complication, the average dose ($\overline{D}$) for measurements with the standard 100 mm pencil chamber and a 160 mm wide cone beam CT scanner was defined:

$$\overline{D}_{100} = \frac{1}{100}\int_{-50\text{ mm}}^{+50\text{ mm}} D(z)\,\mathrm{d}z = \frac{160}{100}\mathrm{CTDI}_{100} \tag{4}$$

where the denominator in the formula for $CTDI_{100}$ is replaced by the actual sensitive length of the ionization chamber (100 mm). A simple relationship exists between $CTDI_{100}$ and $\overline{D}_{100}$ as expressed in the formula. Practically, $\overline{D}_{100}$ expresses the average absorbed dose within the 100 mm pencil ionization chamber. Similarly, for a small thimble Farmer-type ionization chamber with a sensitive length of 24 mm, $\overline{D}_{24}$ expresses the average dose in this chamber, either measured free in air or in a CT dose phantom. The weighted average dose in a CT phantom, $\overline{D}_w$, was calculated using weighting factors of 1/3 and 2/3, respectively, for the centre and the periphery. An even better, although less pragmatic, solution for finding an appropriate dosimetric CTDI metric in 160 mm cone beam CT is to measure $CTDI_{300}$ with an extended pencil chamber (300 mm long) either in extended CT dose phantoms (350 mm long head and body phantoms) (Mori *et al* 2005) or free in air. $CTDI_{300}$ is defined as

$$\mathrm{CTDI}_{300} = \frac{1}{nT}\int_{-150\text{ mm}}^{+150\text{ mm}} D(z)\,\mathrm{d}z. \tag{5}$$

By further extending the integration limits to −300 mm and +300 mm, $CTDI_{600}$ was defined, which was only used in MC simulations (that is, no physical measurements were performed with a 600 mm chamber). Some of the metrics described above for CT dosimetry are graphically presented in figure 1. The dose profile free in air along the *Z*-axis was also characterized by measurements with a small ionization chamber and MC simulations. In these cases, for calculating the CTDI, the integral of $D(z)\,\mathrm{d}z$ was replaced by an appropriate summation of $D(z_i)\,\mathrm{d}$ where $D(z_i)$ is the absorbed dose measured at position z_i and d is the sample distance of the corresponding discrete dose profile.

At this point, a distinction should be made between CTDI and $\overline{D}$. This distinction is necessary as CTDI is meant to represent the average dose from a series of acquisitions (originally a contiguous series of axial acquisitions, and then adopted to helical scans) and therefore has a preferred integration length exceeding the actual cone beam width. This metric should be treated as a fundamentally different dose quantity compared to the average dose ($\overline{D}$) that seeks to represent the average dose from a single axial acquisition (as may be the case with this cone beam scanner) and therefore is associated with measurements entirely within the actual x-ray beam width.

2.3. Dosimetry free in air

Dose measurements were performed free in air to characterize the cone beam along the axis of rotation of the scanner. This was achieved with a thimble Farmer-type ionization chamber (type 2571; volume 0.69 cm^3; length 24.1 mm, inner diameter 6.3 mm, graphite wall; NE Technology Limited, Beenham, Berkshire, UK) connected to a Keithley dosemeter 35050 A (Keithley Instruments, Inc., Cleveland, OH). Consistent performance of the ionization chamber and dosimeter was checked before and after the measurements with a strontium-90 check source (Model 2503; NE Technology Limited, Beenham, Berkshire, UK). The thimble chamber was fixed to the table but in a way that the table did not interfere with the dose measurements. The dose profile along the *Z*-axis was measured by moving the thimble chamber in small steps along the axis of rotation of the scanner (*Z*-axis). The displacements were achieved by horizontal table movement and covered *Z*-axis positions from −150 mm

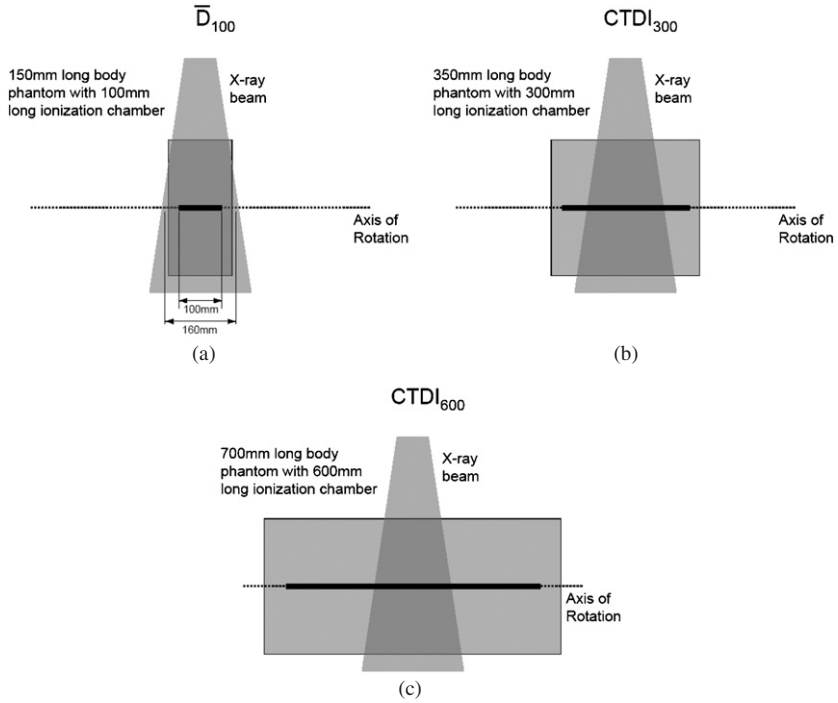

Figure 1. Left: for the calculation of $CTDI_{100}$, the integral of the dose profile is divided by the nominal beam width (160 mm) but the sensitive length of the ionization chamber is much smaller than 160 mm (i.e. 100 mm); this leads to substantial underestimation of $CTDI_{100}$. In this configuration, it is preferable to calculate $\overline{D}_{100}$ as described in section 2.2, in this case better agreement between $\overline{D}_{100w}$ and the $CTDI_w$ metric can be expected. Right: $CTDI_{300}$ can be measured in a 350 mm long CT dose phantom with a 300 mm long ionization chamber (Mori *et al* 2005). Below: $CTDI_{600}$ MC simulations were performed in a simulated 700 mm long CT dose phantom, and the integration length of the dose profile was 600 mm.

to +150 mm. The x-ray rube was fixed (no rotation) at the '12:00 o'clock' location for each table position. To achieve dose measurements free in air with optimal spatial resolution, the cylindrical thimble chamber was orientated with its symmetry axis perpendicular to the *Z*-axis. All measurements of dose profiles with the thimble chamber free in air were performed with a CT technique (tube charge) of 200 mAs (tube current 100 mA, exposure time 2 s, full cone beam). Dose measurements free in air along the axis of rotation of the scanner were also performed with pencil ionization chambers, one standard 100 mm long CT ionization chamber (CapIntec Inc., NJ, USA) and one 300 mm long extended CT pencil ionization chamber (CT-110, Applied Engineering Inc., Japan); these chambers were aligned along the *Z*-axis. All dose measurements free in air with the pencil ionization chambers were performed with a rotating x-ray tube at a CT technique of 300 mAs (tube current 60 mA, exposure time 5 s, full cone beam). From measurements with the 100 mm pencil chamber, both $CTDI_{100air}$ and $\overline{D}_{100air}$ were derived; from measurements with the Farmer-type thimble and 300 mm pencil chamber, $CTDI_{300w}$ was derived. For comparison, the results were compared to previously published results (van der Molen *et al* 2007b) for another MDCT scanner (Aquilion 16, Toshiba Medical Systems, Otawara-shi, Japan). The effect of collimation on CTDI was assessed by measurements with the 300 mm long extended CT pencil ionization chamber for acquisitions with 80–320 active detector rows (in 40 detector row steps), corresponding to a nominal beam

width of 40–160 mm (in 20 mm nominal beam width steps; rotating x-ray tube, large bow tie filter, 120 kV, 60 mA, exposure time 5 s, 300 mAs). Estimated uncertainty in the measurements with ionization chambers was ±5%.

2.4. Dosimetry in CT dose phantoms

Dose measurements with the 100 mm pencil chamber were performed within two standard CT dose phantoms (150 mm long, 160 mm diameter for the head phantom and 320 mm diameter for the body phantom) and with the 300 mm pencil chamber within two extended CT dose phantoms (350 mm long, same diameters as the standard phantoms). The phantoms are PMMA (polymethylmethacrylate) cylinders with holes for insertion of the pencil ionization chambers parallel to the symmetry axis, one hole at the centre and four holes at the periphery at a distance of 10 mm from the surface. The phantoms were positioned on the table with the centre hole coinciding with the *Z*-axis and the peripheral holes coinciding with either the *X*-axis or *Y*-axis. From measurements with the 100 mm pencil chamber, both CTDI_{100w} (equations (2) and (3)) and $\overline{D}_{100w}$ (equations (2) and (4)) were derived; from measurements with the 300 mm pencil chamber, CTDI_{300w} (equations (2) and (5)) was derived. Estimated uncertainty in the measurements with ionization chambers was ±5%.

2.5. Monte Carlo simulations

For MC simulations, ImpactMC software was used (version 1.0, VAMP, Erlangen, Germany). Validation of ImpactMC was performed and results were reported by Deak *et al* (2007). They compared simulated and measured doses within CTDI phantoms, anthropomorphic thorax phantoms (adult and pediatric), an anthropomorphic trunk phantom and an anthropomorphic liver phantom. The measurements were performed with calibrated ionization chambers and thermoluminescent dosimeters. The calculated dose values were generally within 10% of measurements for all phantoms and all investigated conditions. ImpactMC runs a MC simulation to obtain the three-dimensional dose distribution that results from a CT acquisition. The manufacturer of the Aquilion ONE CT scanner (Toshiba Medical Systems) disclosed two measured spectra (120 kV, small and medium bow tie filter) and information about the design of the two bow tie filters. This information was implemented in ImpactMC. Six voxel phantoms, i.e. three CT head dose phantoms (cylindrical phantoms with a length of 150 mm, 350 mm and 700 mm, respectively, and a diameter of 160 mm) and three CT body dose phantoms (same characteristics of the head phantoms but with a diameter of 320 mm), were defined as homogeneous PMMA objects with a density of 1190 mg cm^{-3} surrounded by air. Voxel phantoms had a 512^2 matrix; section thickness was 3 mm for the 150 mm and 350 mm long voxel phantoms and 6 mm for the 700 mm long voxel phantoms. A MatLab script (The MathWorks, Natick, MA, USA) was used to extract dose profiles from the calculated dose distributions that correspond with the centre and peripheral positions within the CT dose voxel phantoms. ImpactMC allows the user to restrict the MC simulation to one interaction; this option was used to calculate the dose distribution that is exclusively associated with interactions directly resulting from the primary beam. This facilitates investigation of the effects of both primary and scattered photons separately, at different positions in the phantom. MC simulations of the dose distribution were also performed for multiple interactions (primary plus scatter). Subtraction of a single interaction dose distribution from a corresponding multiple interaction dose distribution yielded the dose distribution that corresponds with scattered radiation. MC simulations of dose distribution in the phantoms were performed for axial acquisitions (rotating x-ray tube, full rotation, fixed x-ray tube).

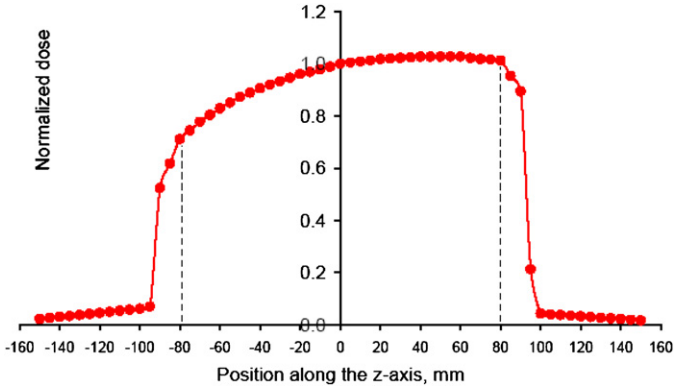

Figure 2. Example of a measured dose profile along the *Z*-axis for a tube voltage of 120 kV and a medium bow tie filter. Dose free in air was measured with a small Farmer-type thimble ionization chamber and dose was normalized to one at $z = 0$.

2.6. Half value layer and nominal beam width

The half value layer was measured for all 12 combinations of tube voltage (four presets) and bow tie filters (three filters) using the thimble chamber and sheets of aluminium, using a non-rotating x-ray tube. Gafchromic XR-QA Dosimetry Film (International Specialty Products Inc. (ISP), Wayne, NJ, USA) was used for measurement of the actual width of the cone beam along the axis of rotation.

3. Results

3.1. Dosimetry free in air

One of the normalized dose profiles that was measured with a small ionization chamber in small steps along the *Z*-axis is shown as an example in figure 2. Table 1 summarizes the results of the dose measurements that were performed to characterize the *Z*-axis dose profile free in air. The results are expressed as $\mathrm{CTDI}_{300\mathrm{air}}$ (equation (5)), $\mathrm{CTDI}_{100\mathrm{air}}$ (equation (3)) and $\overline{D}_{100\mathrm{air}}$ (equation (4)). Correction factors are provided that can be used to derive $\mathrm{CTDI}_{300\mathrm{air}}$ from $\overline{D}_{100\mathrm{air}}$; these factors are calculated by dividing $\mathrm{CTDI}_{300\mathrm{air}}$ by $\overline{D}_{100\mathrm{air}}$. For comparison, $\mathrm{CTDI}_{100\mathrm{air}}$ for a Toshiba Aquilion 16 scanner is also included in the table (van der Molen *et al* 2007a). Figure 3 shows the effect of collimation on $\mathrm{CTDI}_{300\mathrm{air}}$ for nominal beam widths from 40 mm to 160 mm. Values are normalized to $\mathrm{CTDI}_{300\mathrm{air}}$ when the scanner is operated at the full (160 mm) nominal cone beam width.

3.2. Dosimetry in CT dose phantoms

Tables 2 and 3 summarize the results of the dose measurements that were performed in body and head phantoms, respectively. Results are expressed as CTDI_{300w} (equation (5)), CTDI_{100w} (equation (3)) and $\overline{D}_{100w}$ (equation (4)). Correction factors are provided that can be used to derive CTDI_{300w} from $\overline{D}_{100w}$; these values are calculated by dividing CTDI_{300w} by $\overline{D}_{100w}$. CTDI_{100w} values for a Toshiba Aquilion 16 scanner are also included, as a footnote, in the tables.

Table 1. Normalized results of free-in-air dose measurements for the Aquilion ONE scanner (320 × 0.5 mm acquisition configuration) expressed as CTDI and $\overline{D}$ as well as normalized CTDI for the Aquilion 16 scanner (van der Molen *et al* 2007a) (16-detector rows, 0.5 mm section width). Dose measurements were performed with a small thimble chamber, a 100 mm CT pencil chamber and a 300 mm CT pencil chamber. Also in the columns are listed $\overline{D}_{100air}$/mAs correction factors, C_f (shown in parentheses), that can be used to calculate $CTDI_{300air}$ from $\overline{D}_{100air}$ ($CTDI_{300air} = C_f \times \overline{D}_{100air}$).

			Aquilion ONE				Aquilion 16
	Tube voltage (kV)	Bow tie filter	$CTDI_{300air}$/mAs (mGy/mAs)	$CTDI_{300air}$/mAs (mGy/mAs)	$CTDI_{100air}$/mAs (mGy/mAs)	$\overline{D}_{100air}$/mAs (mGy/mAs) (C_f in parentheses)	$CTDI_{100air}$/mAs (mGy/mAs)
Chamber			300 mm pencil	Thimble chamber	100 mm pencil	100 mm pencil	100 mm pencil
Nominal beam width			160 mm	160 mm	160 mm	160 mm	8 mm
Air	80	S	0.117	0.118	0.071	0.114 (1.03)	0.156
Air	100	S	0.198	0.197	0.119	0.190 (1.04)	0.249
Air	120	S	0.295	0.288	0.176	0.281 (1.05)	0.359
Air	135	S	0.375	0.366	0.223	0.357 (1.05)	0.454
Air	80	M	0.101	0.101	0.061	0.098 (1.03)	n.a.
Air	100	M	0.176	0.175	0.106	0.170 (1.04)	n.a.
Air	120	M	0.268	0.263	0.160	0.256 (1.05)	n.a.
Air	135	M	0.344	0.336	0.205	0.329 (1.05)	n.a.
Air	80	L	0.101	0.102	0.062	0.099 (1.02)	0.249
Air	100	L	0.178	0.176	0.107	0.171 (1.04)	0.348
Air	120	L	0.269	0.265	0.161	0.257 (1.05)	0.487
Air	135	L	0.347	0.339	0.206	0.330 (1.05)	0.592

n.a.: not applicable, the Aquilion 16 CT scanner has no medium bow tie filter.

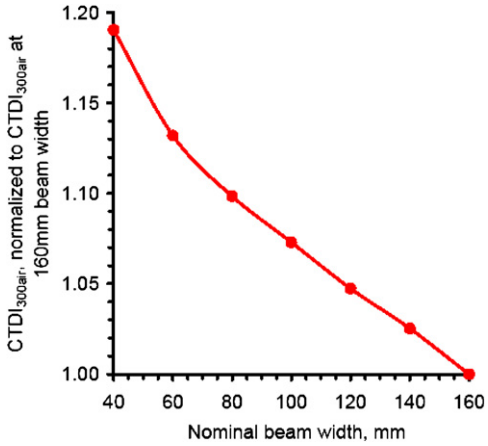

Figure 3. The effect of different nominal beam collimation settings on the $CTDI_{300air}$. Values are normalized to $CTDI_{300air}$ when the scanner is operated at full (160 mm) cone beam width (320 × 0.5 mm acquisition configuration, large bow tie filter, 120 kV).

Table 2. Normalized results of dose measurements in the CT body phantoms for the Aquilion ONE scanner (320 × 0.5 mm acquisition configuration) expressed as CTDI and $\overline{D}$. Dose measurements were performed with a 100 mm CT pencil chamber and a 300 mm CT pencil chamber in 150 mm and 350 mm long CT body phantoms. Also are listed the ratios of $\overline{D}_{100w}$ to $CTDI_{300w}$; correction factors (C_f) are listed in parentheses that can be used to calculate $CTDI_{300w}$ from $\overline{D}_{100w}$ ($CTDI_{300w} = C_f \times \overline{D}_{100w}$).

Tube voltage (kV)	Bow tie	$CTDI_{300w}$/mAs (mGy/mAs)	$CTDI_{100w}$/mAs (mGy/mAs)	$\overline{D}_{100w}$/mAs (mGy/mAs)	$\overline{D}_{100w}/CTDI_{300w}$ (mGy/mGy)
Chamber		300 mm pencil	100 mm pencil	100 mm pencil	(C_f in parentheses)
Phantom length		350 mm	150 mm	150 mm	
80	S	0.032	0.020	0.032	0.98 (1.02)
100	S	0.064	0.039	0.062	0.97 (1.04)
120	S	0.104	0.062	0.099	0.95 (1.06)
135	S	0.140	0.081	0.130	0.93 (1.08)
80	M	0.029	0.018	0.029	1.02 (0.98)
100	M	0.059	0.036	0.058	0.98 (1.02)
120	M	0.098	0.059	0.094	0.96 (1.04)
135	M	0.132	0.078	0.125	0.95 (1.06)
80	L	0.033[a]	0.020	0.032	0.98 (1.02)
100	L	0.066[a]	0.040	0.064	0.96 (1.04)
120	L	0.111[a]	0.064	0.103	0.93 (1.08)
135	L	0.149[a]	0.088	0.141	0.95 (1.06)

[a] For comparison the $CTDI_{100w}$ values for the Toshiba Aquilion 16 (16 sections, section thickness 0.5 mm, CT body phantom length 150 mm): 80 kV 0.053 mGy/mAs; 100 kV 0.094 mGy/mAs; 120 kV 0.142 mGy/mAs; 135 kV 0.189 mGy/mAs. These values should be compared with the values for the large bow tie filter in the table (van der Molen *et al* 2007a).

3.3. Monte Carlo dose simulations

Table 4 shows the results of MC simulations of five CT dose descriptors. Doses are normalized to the $CTDI_{300w}$ (equations (2) and (5)) in the 350 mm long head and body phantoms (bold

Table 3. Normalized results of dose measurements in the CT head phantoms for the Aquilion ONE scanner (320 × 0.5 mm acquisition configuration) expressed as CTDI and $\overline{D}$. Dose measurements were performed with a 100 mm CT pencil chamber and a 300 mm CT pencil chamber in 150 mm and 350 mm long CT head phantoms. Also are listed the ratios of $\overline{D}_{100w}$ to $CTDI_{300w}$; correction factors (C_f) are listed in parentheses that can be used to calculate $CTDI_{300w}$ from $\overline{D}_{100w}$ ($CTDI_{300w} = C_f \times \overline{D}_{100w}$).

Tube voltage (kV)	Bow tie	$CTDI_{300w}$/mAs (mGy/mAs)	$CTDI_{100w}$/mAs (mGy/mAs)	$\overline{D}_{100w}$/mAs (mGy/mAs)	$\overline{D}_{100w}/CTDI_{300w}$ (mGy/mGy)
Chamber		300 mm pencil	100 mm pencil	100 mm pencil	(C_f in parentheses)
Phantom length		350 mm	150 mm	150 mm	
80	S	0.072[a]	0.042	0.067	0.93 (1.08)
100	S	0.136[a]	0.078	0.125	0.91 (1.10)
120	S	0.215[a]	0.122	0.194	0.90 (1.11)
135	S	0.281[a]	0.159	0.254	0.91 (1.10)
80	M	0.066	0.038	0.061	0.93 (1.08)
100	M	0.126	0.072	0.115	0.91 (1.10)
120	M	0.202	0.115	0.183	0.91 (1.10)
135	M	0.265	0.149	0.239	0.90 (1.11)

[a] For comparison the $CTDI_{100w}$ values for the Toshiba Aquilion 16 (16 sections, section thickness 0.5 mm, CT body phantom length 150 mm): 80 kV 0.089 mGy/mAs; 100 kV 0.162 mGy/mAs; 120 kV 0.244 mGy/mAs; 135 kV 0.319 mGy/mAs. These values should be compared with the values for the small bow tie filter in the table (van der Molen *et al* 2007a).

printed values). The results for the head phantom are associated with an acquisition at 120 kV and a small bow tie filter; the results for the body phantom are associated with an acquisition at 120 kV and a medium bow tie filter. Table 5 provides detailed information of MC dose simulations and dose measurements at different positions within the CT body phantom; the results apply to acquisitions at 120 kV and a medium bow tie filter (for the body phantom) and 120 kV and a small bow tie filter (for the head phantom). Doses are normalized to the $CTDI_{300w}$ (bold printed values). Figure 4 shows calculated dose profiles for the 350 mm long body phantom resulting from an axial acquisition (120 kV, medium bow tie filter, full beam, full rotation of the x-ray tube, no table movement). Normalized dose profiles correspond to the primary (a), scattered (b) and total beam (c), respectively.

3.4. Half value layer and nominal beam width

Measurements with film yielded an actual beam width (FWHM) of 180 mm at the centre of rotation which is in agreement with the dose profiles measured with the small ionization chamber. In table 6 are listed the measured (first and second) half value layers (measured at the centre of the cone beam).

4. Discussion

4.1. Dosimetry free in air

$CTDI_{300air}$ was used as a standard of reference for the evaluation of our measurements and calculations. For measurements free in air, this is considered appropriate since the chamber is much longer compared to the primary beam width, and the contribution of (scattered) radiation is very low. Dose profiles measured free in air along the *Z*-axis show a slight gradient (figure 2), resulting from the anode heel effect. The actual measured FWHM of the cone beam (180 mm) slightly exceeds the nominal beam width due to the penumbra. The manufacturer has

Table 4. Results of the MC simulations for the Aquilion ONE CT scanner (320 × 0.5 mm acquisition configuration) for a CT dose head phantom (120 kV, small bow tie) and a CT dose body phantom (120 kV, medium bow tie). Five dose descriptors ($\overline{D}_{24w}$, $\overline{D}_{100w}$, $CTDI_{100w}$, $CTDI_{300w}$ and $CTDI_{600w}$) are derived from the calculated dose distribution in the CT dose phantoms. Doses are normalized to $CTDI_{300w}$ in the 350 mm long CT dose phantoms (bold values).

	Phantom length (mm)		
	150	350	700
Head phantom, 120 kV, small bow tie			
$\overline{D}_{24w}$	0.91	0.93	0.93
$\overline{D}_{100w}$	0.89	0.91	0.91
$CTDI_{100w}$	0.55	0.57	0.57
$CTDI_{300w}$	n.a.	**1.00**	0.99
$CTDI_{600w}$	n.a.	n.a.	1.01
Body phantom, 120 kV, medium bow tie			
$\overline{D}_{24w}$	0.99	1.02	1.01
$\overline{D}_{100w}$	0.95	0.99	0.99
$CTDI_{100w}$	0.59	0.62	0.62
$CTDI_{300w}$	n.a.	**1.00**	0.99
$CTDI_{600w}$	n.a.	n.a.	1.04

Table 5. Results of MC simulations and dose measurements for the Aquilion ONE CT scanner (320 × 0.5 mm acquisition configuration) for the CT dose head phantom (120 kV, small bow tie) and the CT dose body phantom (120 kV, medium bow tie). Three dose descriptors ($\overline{D}_{100}$, $CTDI_{100}$ and $CTDI_{300w}$) are derived from the calculated and measured dose distribution in the CT dose phantoms. Doses are provided for the centre and peripheral positions in the phantoms, in addition the weighted dose is listed in the table. Doses are normalized to $CTDI_{300w}$ in the 350 mm long CT dose phantoms (bold values).

	Calculated values (Monte Carlo simulations)			Measured values (Ionization chambers)		
	$\overline{D}_{100}$	$CTDI_{100}$	$CTDI_{300}$	$\overline{D}_{100}$	$CTDI_{100}$	$CTDI_{300}$
Phantom length (mm)	150	150	350	150	150	350
Body phantom, 120 kV, medium bow tie filter						
Weighted	0.95	0.59	**1.00**	0.98	0.61	**1.00**
Centre	0.59	0.37	0.82	0.58	0.36	0.78
Periphery	1.12	0.70	1.09	1.18	0.74	1.11
Head phantom, 120 kV, small bow tie filter						
Weighted	0.89	0.55	**1.00**	0.91	0.57	**1.00**
Centre	0.79	0.49	0.95	0.81	0.51	0.97
Periphery	0.94	0.59	1.02	0.96	0.60	1.02

stated that the actual beam width will decrease in the near future, coming closer to the nominal beam width. As could be expected, there is excellent correspondence between measurements of $CTDI_{300air}$ performed with the 300 mm long pencil chamber and $CTDI_{300air}$ derived from the measured dose profile with the thimble chamber. $CTDI_{300air}$ can, as could be expected, be derived relatively easy from measurements of the dose profile with the widely available small Farmer-type ionization chamber. Also as expected, $CTDI_{100air}$ derived from measurements with the 100 mm pencil chamber substantially underestimates $CTDI_{300air}$; however, $\overline{D}_{100air}$ is only slightly lower compared to $CTDI_{300air}$. Measurement of $\overline{D}_{100air}$ with the standard 100 mm long pencil only underestimates $CTDI_{300air}$ by 2–5%, and thus $\overline{D}_{100air}$ could be

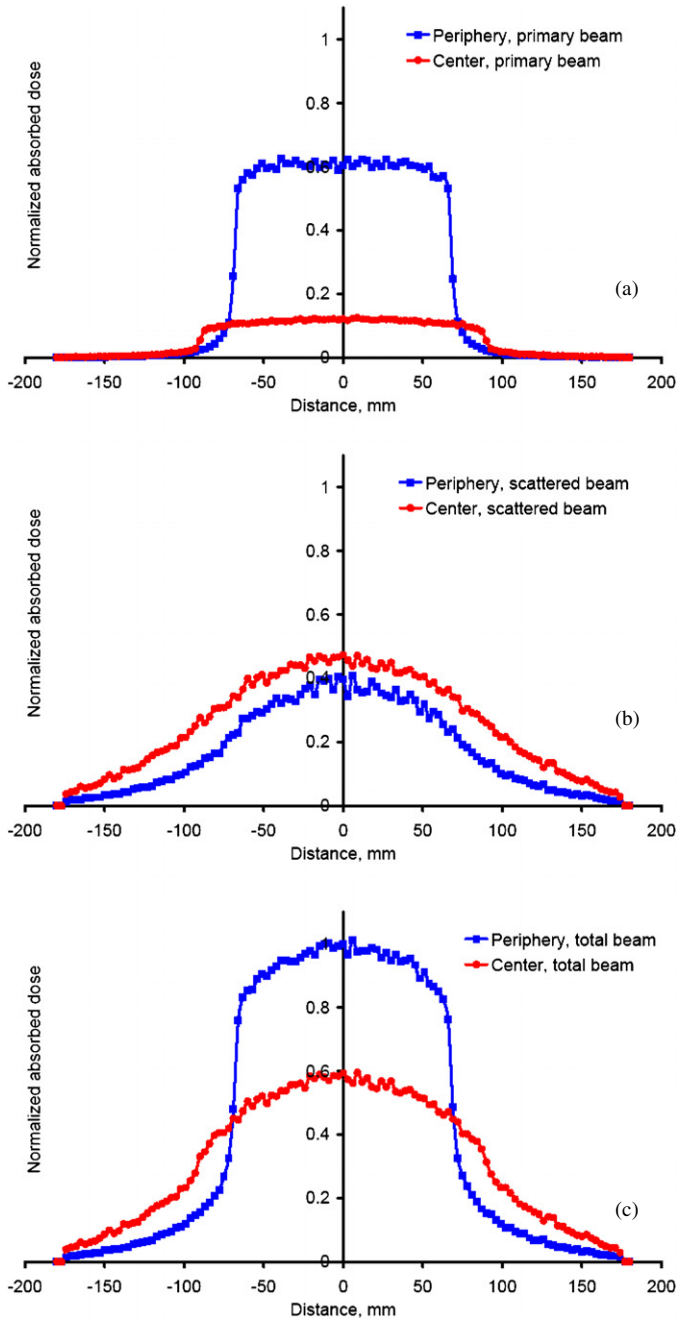

Figure 4. Calculated (simulated) dose profiles for an axial acquisition (full rotation) in the 350 mm long CT body phantom (120 kV, medium bow tie, above). Dose profiles correspond to the primary (a), scattered (b) and total beam (c). Each graph shows dose profiles for the centre position and the peripheral position. The acquisition configuration was 320 × 0.5 mm. Results were normalized to the dose for the total beam at the $z = 0$ peripheral position. Characteristic for the primary beam is the lack of tails of scattered radiation (a); the smooth shape (b) is characteristic for scattered radiation; (c) shows the sum of primary and scattered radiation.

Table 6. First and second half value layers (HVL), expressed in equivalent mm of Al, for four tube voltages and three bow tie filters. Note that the Al equivalent for the second HVL is the amount of additional (not total) filtration beyond that required to obtain the first HVL.

	Small bow tie filter	Medium bow tie filter	Large bow tie filter
80 kV			
First HVL	4.3	4.7	4.7
Second HVL	5.3	6.2	6.2
100 kV			
First HVL	5.4	5.8	5.8
Second HVL	6.8	8.1	8.2
120 kV			
First HVL	6.4	6.9	7.1
Second HVL	8.7	9.7	9.6
135 kV			
First HVL	7.2	7.7	7.7
Second HVL	9.4	10.3	10.3

considered appropriate for assessing the dose in air for the Aquilion ONE CT scanner. It should be noted that this table shows that the measured $CTDI_{300air}$ for the Aquilion ONE scanner is substantially lower than the published $CTDI_{100air}$ for the 16 × 0.5 mm detector configuration on an Aquilion 16 scanner.

Figure 3 shows the effect of nominal beam width on the $CTDI_{300air}$. The trend in the figure expresses the well-known phenomenon that a smaller beam width, or less active detector rows, results in a higher CTDI due to the relatively larger contribution of the penumbra to CTDI.

4.2. Dosimetry in CT dose phantoms

Mori *et al* (2005) concluded that the required phantom length and integration length for a 256 detector row cone beam scanner with a nominal beam width of 128 mm needed to be at least 300 mm. Their findings support the standard of reference that was used in this study, i.e. 350 mm long phantoms in combination with a 300 mm long pencil ionization chamber.

For the body phantom, there is good correspondence between measured $CTDI_{300w}$ in the extended CT dose body phantom and $\overline{D}_{100w}$ measured with the 100 mm pencil chamber in the standard (150 mm long) CT dose phantom. This is illustrated in table 2 by the ratio of $CTDI_{300w}$ to $\overline{D}_{100w}$ that comes close to unity under all conditions. In general, $CTDI_{300w}$ is only slightly underestimated by $\overline{D}_{100w}$. The values between brackets are correction factors that can be used to derive $CTDI_{300w}$ from measurement of $\overline{D}_{100w}$; the correction factors are within a small range, varying between 0.98 and 1.08. The table also shows that $CTDI_{100w}$ substantially underestimates $CTDI_{300w}$ as expected.

For the head phantom, there is also good correspondence between measured $CTDI_{300w}$ in the extended CT dose head phantom and $\overline{D}_{100w}$ measured with the 100 mm pencil chamber in the (150 mm long) standard CT dose phantom (table 3). This is demonstrated by the ratio values in the last column that are close to unity. Correction factors that can be used to derive $CTDI_{300w}$ from measurement of $\overline{D}_{100w}$ for the head phantom are only slightly larger than those obtained for the body phantom, varying between 1.08 and 1.11. $CTDI_{100w}$ substantially underestimates $CTDI_{300w}$. For both the 150 mm long CT head and CT body phantom, measurement of $\overline{D}_{100w}$ can be considered as a good approximation of the actual $CTDI_{300w}$. $CTDI_{300w}$ can be assessed even more accurately from $\overline{D}_{100w}$ by application of a small correction factor.

Similar to $CTDI_{100air}$, published $CTDI_{100w}$ for the 16 × 0.5 mm detector configuration on the Toshiba Aquilion 16 scanner is substantially higher compared to measured $CTDI_{300w}$ ($CTDI_{300air}$) for the Aquilion ONE scanner. This may be attributable to the different designs of the bow tie filters of these two scanners and possibly, to a lesser extent, to a relatively larger contribution of penumbra at the Aquilion 16 scanner. This demonstrates that the output of the two scanners is different for the Aquilion ONE scanner compared to the Aquilion 16 CT scanner (this is also true for the Aquilion 4 and 64 CT scanners since these scanners use the same bow tie filters as the Aquilion 16 CT scanner). Therefore, acquisition protocols for the Aquilion ONE should not derive their mAs values directly from acquisition protocols of the previous generation of Aquilion CT scanners as their designs (and outputs) are noticeably different. Differences in $CTDI_w$/mAs in itself obviously do not provide any indication of patient dose; patient dose depends on the actual clinically applied tube current and rotation time in combination with the $CTDI_w$/mAs and the selected tube voltage.

4.3. Monte Carlo dose simulations

Results for simulated very long phantoms (700 mm) and a very long integration length (600 mm) in table 4 correspond well with our standard of reference, namely the 350 mm long phantoms and 300 mm dose profile integration length. This is in agreement with findings from another study (Mori *et al* 2005) where they also observed that measurement with the 300 mm long ionization chamber and 350 mm long phantoms provides an appropriate and accurate methodology for assessment of CTDI in phantoms and a cone beam scanner.

Assessment of $\overline{D}_{24w}$, which can be measured with a small Farmer-type ionization chamber, yields very consistent results even when phantoms of different lengths are being used. $\overline{D}_{24w}$ simulated in a 150 mm long body phantom only underestimates $CTDI_{300w}$ (in 350 mm long phantoms) by 1%; in a head phantom the underestimation is 9%. $\overline{D}_{24w}$ yields consistently slightly higher values when compared to $\overline{D}_{100w}$, possibly due to a slightly higher contribution of scattered radiation at the middle part of the phantom which systematically turns in favour of $\overline{D}_{24w}$. These findings support the potential benefit of point dose measurements in CT dosimetry as already suggested by Dixon and Ballard (2007); table 5 shows that the calculated (simulated) results accurately reproduce the measured results for $\overline{D}_{100w}$ and $CTDI_{100w}$.

Whereas good correspondence between $CTDI_{300w}$ and $\overline{D}_{100w}$ was found, a detailed review of $CTDI_{300}$ and $\overline{D}_{100}$ at different positions within the head and body phantoms revealed considerable differences (table 5). At the centre position in the 150 mm long phantom, average dose ($\overline{D}_{100centre}$) is much lower compared to CTDI in the 350 mm long phantom ($CTDI_{300centre}$). This could be expected since the large integration length that is associated with $CTDI_{300}$ and the longer phantom length result in a larger contribution of scattered radiation (and penumbra) to $CTDI_{300}$ compared to $\overline{D}_{100}$. A less obvious observation was that, in the head phantom, the measured and calculated average doses at the peripheral positions ($\overline{D}_{100periphery}$) are only slightly lower compared to CTDI ($CTDI_{300periphery}$), and that, in the body phantom, average dose ($\overline{D}_{100periphery}$) even exceeds CTDI at the peripheral position ($CTDI_{300periphery}$). The relatively high weighting factor for the peripheral positions and the rather good correspondence between $CTDI_{300periphery}$ and $\overline{D}_{100periphery}$ result in surprisingly good agreement between $CTDI_{300w}$ and $\overline{D}_{100w}$. $CTDI_{100}$ clearly underestimates $CTDI_{300}$ at all measurement positions within the phantoms. The good correspondence between measured values (ionization chambers) and calculated values (MC) in table 5 confirms appropriate performance of the MC modelling.

Seemingly surprising observations with regard to average dose and CTDI at different positions within the CT dose phantoms will be explored further by analysis of calculated dose profiles in the CT body phantom resulting from an axial acquisition (full rotation, full cone

beam, 120 kV, medium bow tie filter). Figure 4 shows normalized dose profiles corresponding to the primary, scattered and total beam for both the centre and peripheral positions in the body phantom. For the primary beam, the FWHM of the centre profile accurately corresponds with the actual 180 mm cone beam width whereas the peripheral profile is much smaller, i.e. 137 mm (figure 4(a)). The same pattern of a larger FWHM for the centre profile can be observed in the scattered beam (figure 4(b)) and the total beam (figure 4(c)). This suggests that geometrical aspects play a considerable role. The resulting dose profiles at the peripheral position for the total beam are higher within the range of the nominal beam width, and lower at the tails. The main reason for this is that the peripheral position accumulates more of its radiation dose from non-scattered radiation, whereas the centre position accumulates more of its dose from scattered radiation.

The observed differences in figure 4 for the centre and peripheral profile widths can be explained from geometrical considerations. During a full rotation, the actual (primary) cone beam width remains constant at the centre position and consequently the observed dose profile accurately corresponds with the actual (primary) cone beam width of 180 mm at the centre of rotation. However, at the peripheral positions, during a full rotation, the actual (primary) cone beam width changes between 135 mm and 225 mm (from when the x-ray source is directly over the location to when it is 180° or half a rotation away); these values follow simply from the geometry of the CT dose body phantom and the focus to centre-of-rotation distance of 600 mm. The by far predominant contribution to the dose profile at a peripheral position is when the focal spot is closest to that peripheral position; in this case the actual (primary) beam width is at its smallest (135 mm). This explains the observed relatively small dose profiles at the peripheral positions. This geometric phenomenon strongly affects CTDI ($CTDI_{300periphery}$), but does not affect average dose ($\overline{D}_{100periphery}$), since its integration length of 100 mm is always smaller than the variable (primary) cone beam width, and at each tube angle, the entire ionization chamber is exposed. These geometric effects play a less dominant role in the head phantom, simply because of its smaller diameter (and the relative cone beam widths only range from 185 to 195 mm from closest to further position from the x-ray source). In conclusion, the variable (primary) cone beam width at the peripheral position introduces a systematic effect in favour of $\overline{D}_{100periphery}$ compared to $CTDI_{300periphery}$ ($\overline{D}_{100periphery} > CTDI_{300periphery}$), most prominently for the body phantom.

4.4. Dose quantities in CT

Two fundamental differences between the quantities CTDI ($CTDI_{300}$) and average dose ($\overline{D}_{100}$) should be considered. First, $CTDI_{300}$ inherently takes into account contributions from the tails of the dose distribution extending beyond the nominal beam width (of 160 mm at the centre of rotation), and it is measured in an extended CT dose phantom. $\overline{D}_{100}$ is the average dose along a relatively small range entirely within the primary beam and is measured in a standard sized CT dose phantom. At first sight, this should introduce a bias in favour of $CTDI_{300}$ compared to $\overline{D}_{100}$ ($CTDI_{300} > \overline{D}_{100}$), which was actually observed for the centre positions in table 5. On the other hand, the variable (primary) cone beam width at the peripheral position introduces a bias in favour of $\overline{D}_{100}$ compared to $CTDI_{300}$ which was actually observed for the peripheral positions in table 5.

The fact that $CTDI_{300}$ is calculated by dividing by the total width of all acquired sections makes $CTDI_{300}$ a fundamentally different dose descriptor compared to the (average) absorbed dose ($\overline{D}_{100}$). This is illustrated by assuming a static exposure condition (a fixed x-ray tube) and dose measurement under scatter-free conditions. Under these conditions, $\overline{D}_{100}$ within the cone beam increases with decreasing distance (d, mm) to the focus according to the

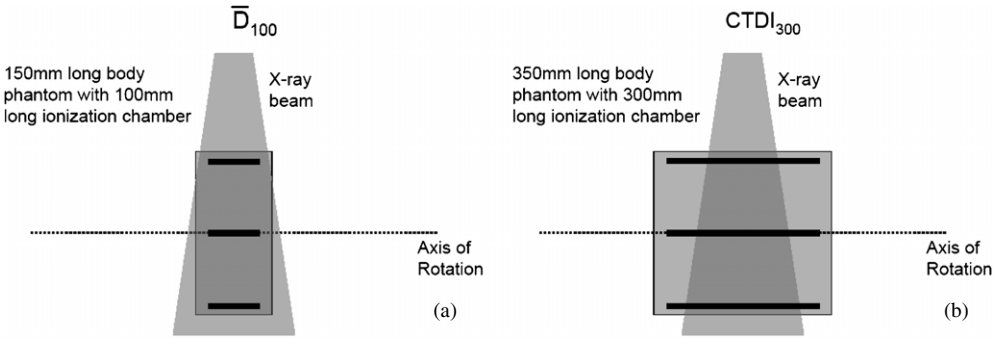

Figure 5. Illustration of geometrical aspects of dosimetry with a 320-detector row, 160 mm wide cone beam CT scanner: (a) shows that the extent of the dose integral covering the primary (nominal) beam width is constant (i.e. 100 mm) at different positions within the phantom when the standard 150 mm long CT dose body phantom is used in combination with a 100 mm long ionization chamber; (b) shows that the extent of coverage of the primary beam by the dose integral depends strongly on the position of the ionization chamber in the phantom and the position of the x-ray tube when the 350 mm long CT dose phantom is used in combination with a 300 mm long ionization chamber.

well-known inverse square law ($D \sim 1/d^2$). The length of the 300 mm pencil chamber that is exposed to the x-ray beam (l, mm) decreases with decreasing distance from the focus. There is a simple linear relationship between the exposed length and distance to the focus ($l \sim d$). Dose measurements with a 300 mm pencil ionization chamber are affected by both the inverse square law and the linear relation between exposed length and distance. Consequently (under scatter-free conditions), measurements of $\overline{D}_{100}$ at closer distances to the focus increase as a quadratic function, whereas CTDI_{300} only increases linearly when the chamber moves towards the focus. CTDI_{300} and $\overline{D}_{100}$ thus behave as fundamentally different dose descriptors. Although the presented CTDI_{100} for the cone beam scanner was calculated strictly according to the definition of CTDI, the preceding considerations indicate that CTDI_{100} should probably not be used for this purpose.

Taking into account that the major contribution to the peripheral measurements occurs at an exposure geometry when the tube is closest to the measurement chamber, it can be concluded that the relative reading of $\overline{D}_{100\mathrm{periphery}}$ (where under scatter-free conditions is proportional to $1/d^2$) is more strongly affected by the distance d to the focus compared to $\mathrm{CTDI}_{300\mathrm{periphery}}$ (where under scatter-free conditions is proportional to $1/d$). This explains, at least in part, the observed relatively high $\overline{D}_{100\mathrm{periphery}}$ readings. Measurements of CTDI_{300w} and $\overline{D}_{100w}$ only yielded similar results since in the weighting substantially more weight is assigned to the readings in the peripheral positions, which particularly favours $\overline{D}_{100w}$.

Figure 5 illustrates some geometrical aspects of dosimetry with a wide cone beam CT scanner. The extent of the dose integral of the primary beam is constant at different positions within the phantom when the standard 150 mm long CT dose body phantom is used in combination with a 100 mm long ionization chamber. However, the extent of the dose integral of the primary beam depends strongly on the position of the ionization chamber in the phantom and the position of the x-ray tube when the 350 mm long CT dose phantom is used in combination with a 300 mm long ionization chamber.

The dose descriptor dose length product (DLP) can easily be derived from CTDI_{300w} by multiplication with the total width of all acquired sections. For an axial cone beam acquisition, this DLP is in fact the weighted integral of dose profiles ($D(z)$, centre and peripheral integrals)

within a CT dose phantom. A rough approximation of DLP (mGy cm) can also be derived by multiplication of $\overline{D}_{100w}$ (mGy) by the total width of all acquired sections (cm).

Assessment of the effective dose is more complicated. One could consider using published DLP to effective dose conversion factors (Huda *et al* 2008, Jessen *et al* 1999), or perhaps one of the programs that are available for effective dose assessment from CTDI free in air, after appropriate scanner matching (McCollough 2003, Shrimpton & Edyvean 1998, Zankl *et al* 1991). However, the accuracy of such approaches should be verified, preferably through dedicated MC simulations of the dose distribution in either anthropomorphic mathematical or voxel phantoms for the Aquilion ONE cone beam CT scanner.

4.5. Half value layer and nominal beam width

The proposed methodology of using a 100 mm chamber and 150 mm long CT dose phantoms for assessment of $\overline{D}_{100}$ does not allow for assessment of the outer limits of the (primary) dose profile whereas CTDI_{300} explicitly does. Thus, in combination with a pragmatic assessment of $\overline{D}_{100}$, one should always verify that the primary cone beam width, including penumbra, is similar to the beam width for the Aquilion ONE scanner at which the 300 mm chamber 'standard of reference' measurements were performed. This can be achieved either by measuring the dose profile free in air with a small ionization chamber (Jansen *et al* 1996) or even more conveniently by relative dosimetry with film (Gorny *et al* 2005) or OSL's (Bauhs *et al* 2008).

In addition to assessment of dose descriptors, an evaluation of the half value layer provides an effective measure for checking the appropriate characteristics of the x-ray beam of CT scanners. In table 6 are provided half value layers for all possible combinations of tube voltage and bow tie filter to facilitate such evaluations. As could be expected, half value layers increase with increasing tube voltage. Half value layers for the small bow tie filter are slightly lower compared to the medium and large bow tie filters.

5. Conclusions

In conclusion, a pragmatic methodology for dosimetric assessment of a wide cone beam CT scanner, based on CTDI_{300}, could start with measurement of the average dose ($\overline{D}_{100w}$) with readily available equipment. Factors can be used to correct for the (modest) differences between $\overline{D}_{100w}$ and CTDI_{300} (see tables 2 and 3) and for the difference between a collimated beam and a full cone beam (see figure 3).

Fundamental considerations warrant against assessment of CTDI for a 320 detector row CT scanner according to the currently used dosimetric CTDI metrics that are based on 100 mm long pencil chambers in combination with the 150 mm long CT dosimetry phantoms, such results are preferably expressed as the average dose ($\overline{D}$). To fulfil the requirement that a sufficiently accurate CTDI is calculated from an integration of at least the entire (primary) beam dose profile within phantoms that exceed the nominal beam width, dose measurements with a 300 mm long pencil chamber in combination with 350 mm long phantoms are proposed. This seems an appropriate solution since longer phantoms and a longer integration length do not substantially improve the assessment of CTDI for the Aquilion ONE 320 detector row CT scanner. The beam characteristics of the investigated CT scanner, especially the dose tails extending the width of the 100 mm pencil chamber, should be explored also in order to verify that the beam width of the investigated scanner correspond adequately with the scanner for which the correction factors have been established. Geometrical considerations provide an explanation of the fundamental discrepancies that are observed between CTDI_{300} and $\overline{D}_{100}$

at the peripheral positions within the CT dose phantoms. In general, any CTDI value that is derived from a dose profile extending the beam width is fundamentally different from a dose descriptor that is derived from dose measurements exclusively within the x-ray beam. This conclusion is also of relevance for other applications of dosimetry, e.g. in 3D imaging with C-arms or dedicated cone beam CT for dental applications. To support the differentiation between the two different CT dose descriptors, different symbols and quantities, e.g. $CTDI_{300}$ and $\overline{D}_{100}$, are proposed

The herewith proposed methodology can fill the gap between existing metrics in CT dosimetry and better optimized metrics for CT that should be developed in the future. Clearly, CTDI was intended for use in axial or helical fan beam CT, were CTDI integrates tails of adjacent axial or helical rotations. Adjacent rotations are of less importance in wide cone beam axial CT, since sometimes only one axial acquisition provides sufficient anatomical coverage, although sometimes in wide cone beam CT also multiple axial acquisitions have to be performed and combined in the reconstruction process by stitching. Technical developments in CT and practical considerations already necessitated numerous modifications in the CTDI metric, as its introduction was based on axial acquisitions, measurement of absorbed dose in acrylic and an integration length of ± 7 times the nominal slice width. Subsequently, most important modifications included expression of CTDI as an absorbed dose in air, fixing the integration length to 100 mm, weighting the CTDI at centre and peripheral position with factors of $1/3$ and $2/3$, respectively, and adapting CTDI to helical acquisitions ($CTDI_{volume}$). There is a strong tendency towards increasing use of wide cone beam CT. Dedicated wide cone beam scanners have become available for general diagnosis, like the scanner that was evaluated in this study, but also for dental applications (dental CT scanners). With modern equipment, additional 3D imaging with flat panel detectors is becoming available for medical doctors performing fluoroscopy guided interventions, e.g. for mobile and fixed C-arm units equipped with flat panel detectors. Practical considerations will probably show that it is not appropriate to adapt CTDI again to make this metric applicable for routine clinical dosimetry at such new scanners since this would require large-scale implementation of dosimetry with longer pencil ionization chambers and extended CT dose phantoms. It is clear that CT dosimetry has to be adapted fundamentally for application in wide cone beam CT and that completely new dose metrics should be considered. Suitable candidates for new metrics in CT dosimetry could be based on point dose measurements in a phantom (in line with the methodology applied in this study); but also implementation of dose area product in CT, analogous as in radiography and fluoroscopy, could be considered as a measure to quantify the output of CT.

Acknowledgments

We thank Y Saito, M Kazama, Ms M Okumura (Toshiba Medical Systems), and H de Vries (Toshiba Medical Systems Europe) for providing spectral information and the bow tie filter design and for their assistance with the dose measurements.

References

Bauhs J A, Vrieze T J, Primak A N, Bruesewitz M R and McCollough C H 2008 CT dosimetry: comparison of measurement techniques and devices *Radiographics* **28** 245–53

Deak P, van S M, Shrimpton P C, Zankl M and Kalender W A 2007 Validation of a Monte Carlo tool for patient-specific dose simulations in multi-slice computed tomography *Eur. Radiol.* **18** 759–72

Dewey M, Zimmermann E, Laule M, Rutsch W and Hamm B 2008 Three-vessel coronary artery disease examined with 320-slice computed tomography coronary angiography *Eur. Heart J.* **29** 1669

Dixon R L and Ballard A C 2007 Experimental validation of a versatile system of CT dosimetry using a conventional ion chamber: beyond CTDI100 *Med. Phys.* **34** 3399–413

FDA 2006 *Guidance for Industry, FDA Staff and Third Parties—Provision for Alternate Measure of the Computed Tomography Dose Index (CTDI) to Assure Compliance with the Dose Information Requirements of the Federal Performance for Computed Tomography* US Food and Drug Administration (FDA)

Gorny K R, Leitzen S L, Bruesewitz M R, Kofler J M, Hangiandreou N J and McCollough C H 2005 The calibration of experimental self-developing Gafchromic HXR film for the measurement of radiation dose in computed tomography *Med. Phys.* **32** 1010–6

Huda W, Ogden K M and Khorasani M R 2008 Converting dose-length product to effective dose at CT *Radiology* **248** 995–1003

IEC 2002 Medical electrical equipment: Part 2-44. Particular requirements for the safety of x-ray equipment for computed tomography *IEC 60601-2-44*

Jansen J T, Geleijns J, Zweers D, Schultz F W and Zoetelief J 1996 Calculation of computed tomography dose index to effective dose conversion factors based on measurement of the dose profile along the fan shaped beam *Br. J. Radiol.* **69** 33–41

Jessen K A, Shrimpton P C, Geleijns J, Panzer W and Tosi G 1999 Dosimetry for optimisation of patient protection in computed tomography *Appl. Radiat. Isot.* **50** 165–72

McCollough C H 2003 Patient dose in cardiac computed tomography *Herz* **28** 1–6

McNitt-Gray M F 2002 AAPM/RSNA physics tutorial for residents: topics in CT. Radiation dose in CT *Radiographics* **22** 1541–53

Mori S, Endo M, Nishizawa K, Tsunoo T, Aoyama T, Fujiwara H and Murase K 2005 Enlarged longitudinal dose profiles in cone-beam CT and the need for modified dosimetry *Med. Phys.* **32** 1061–9

Rybicki F J *et al* 2008 Initial evaluation of coronary images from 320-detector row computed tomography *Int. J. Cardiovasc. Imaging* **24** 535–46

Shope T B, Gagne R M and Johnson G C 1981 A method for describing the doses delivered by transmission x-ray computed tomography *Med. Phys.* **8** 488–95

Shrimpton P C and Edyvean S 1998 CT scanner dosimetry *Br. J. Radiol.* **71** 1–3

Van Der Molen A J, Veldkamp W J and Geleijns J 2007a 16-slice CT: achievable effective doses of common protocols in comparison with recent CT dose surveys *Br. J. Radiol.* **80** 248–55

Van Der Molen A J, Veldkamp W J and Geleijns J 2007b 16-slice CT: achievable effective doses of common protocols in comparison with recent CT dose surveys *Br. J. Radiol.* **80** 248–55

Zankl M, Panzer W and Drexler G 1991 The calculation of dose from external photon exposures using reference human phantoms and Monte Carlo methods: Part VI. Organ doses from computed tomographic examinations *GSF-Bericht 30/91* (Neuherberg, Germany: Gesellschaft für Strahlen- und Umweltforschung)